A Software Tool for the Computation of Arterial Pulse Wave Velocity from Flow-sensitive 4D MRI Data

J Drexl[1], H Mirzaee[1], A Harloff[2], M Hüllebrand[1], A Hennemuth[1], H Hahn[1]

[1]Fraunhofer MEVIS, Bremen, Germany
[2]Department of Neurology, University Hospital, Albert-Ludwigs-Universität Freiburg, Germany

Abstract

Recently, Markl at al. [1] demonstrated that the aortic pulse wave velocity (PWV) can be measured non-invasively based on flow-sensitive 4D MRI. However, the suggested post-processing workflow is very time consuming. In this paper, we present a more efficient PWV computation integrated into a dedicated software assistant, supporting all major steps for PWV computation. The implementation was validated on a digital phantom. Furthermore, two independent observers re-processed the volunteer data from the Markl et al. study with our software, so that outcomes as well as processing times could be compared. The implementation of our method gives similar accuracy and reproducibility to the method of Markl at al, but at a significantly reduced processing time.

1. Introduction

Measurement of aortic pulse wave velocity (PWV) is of high clinical importance, as increased aortic PWV is a surrogate marker for reduced vessel wall elasticity. Vessel wall elasticity changes due to aging and also to development of atherosclerosis.

The gold standard approach for determining PWV is to use a pressure catheter. However, this procedure is invasive and requires radiation and exposition to iodine-based contrast agents. An established approach for the non-invasive measurement of PWV is based on 2D CINE phase contrast magnetic resonance imaging data [2]. While the approach yields accurate results, there is the drawback of the labor intensive manual placement of analysis planes on the MRI scanner and the inability to measure PWV in complex aortic geometries [1].

An alternative to 2D PCMRI is velocity-encoded tridirectional phase-contrast magnetic resonance imaging (4D flow MRI). 4D flow MRI is especially attractive, because unlike 2D CINE PCMRI the manual placement of analysis planes before scanning is not necessary. A full 4D velocity field is acquired, thus parameters such as flow rate velocity curves, pressure maps, and wall shear stress (WSS) can be calculated from the raw data in a retrospective fashion. Similarly, 4D flow MRI offers the prospect of offline PWV calculation from the full 4D velocity field in a highly automated manner. However, 4D flow MRI is restricted by the coarser resolution in contrast to 2D PC-MRI, and time resolution is a critical parameter for an accurate measurement of PWV. In a recent study by Markl et al. [1], it was shown that the volumetric coverage of 4D flow MRI can compensate for its lower temporal resolution. They demonstrated that PWV can be reliably derived based on 4D PCMRI data by computing the PWV from more than 30 analysis planes that are distributed along the thoracic aorta. They obtained results comparable to the methods based on 2D PCMRI data. In their approach, observers interactively placed analysis planes along the aorta. In each analysis plane, the boundaries of the aortic lumen were manually delineated. Then, for every analysis plane, a flow rate curve was computed. Finally, the PWV along the entire thoracic aorta was calculated from the ensemble of flow rate curves by the time-to-foot (TTF), time-to-peak (TTP) and cross-correlation (XCor) methods [1]. One major drawback of that study was the enormous effort needed for data analysis, which was in the order of three hours per patient. For a broader application in large study trials or clinical routine, PWV calculation should be as fast as possible.

2. Method

We built upon the study by Markl et al. [1] by providing an automatic generation of the regions of interest for the flow rate curve computation. Our method requires only a 3D segmentation of the aorta and the manual specification of a start and end point along the course of the aorta (Fig. 1). The PWV computation algorithm is described in detail in Table 1. Although in the last step of the algorithm different choices for extracting the pulse wave velocity from the flow curves can be made, in this study we solely employed the time-to-foot criterion to allow comparison to the results

of Markl et al [1]. As suggested in [1], the "foot" point is defined as the intersection of a secant line to the upslope portion of the flow curve with the abscissa. The secant is placed between 20% and 80% of the peak flow.

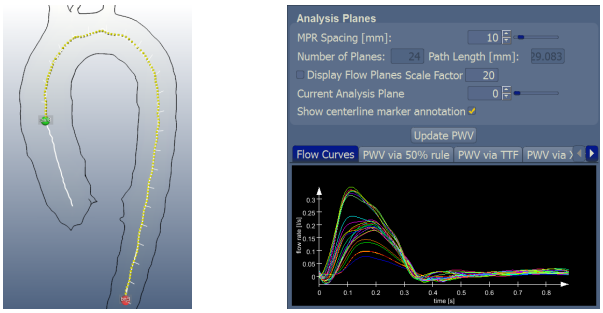

a) Centerline b) PWV module

Figure 1. Screenshot implementation of PWV module.

Contrary to [1], the manual effort for this approach is independent of the spatial distance Δs between the analysis planes, thus PWV can be easily computed using a finer Δs than the 1 cm value used in [1]. Furthermore, we have fully integrated the PWV computation into a software assistant [3], thereby supporting the full workflow starting with data import, velocity offset error correction, phase unwrapping, semi-automatic segmentation of the aorta, and finally PWV computation.

Input:
Velocity field $\mathbf{v}(\mathbf{x}, t)$, vessel mask $m(\mathbf{x})$, start/endpoint.
Output:
Pulse wave velocity c.

Pseudocode:
1) Shrink vessel mask $m(\mathbf{x})$ to a fixed percentage ϵ of it's original size.
2) Extract centerline from mask.
3) Equidistantly (distance Δs) traverse the centerline to get oriented analysis planes with normal $\mathbf{n}_k$.
4) Intersect analysis planes with mask: get oriented contours A_k.
5) For each analysis plane k compute flow rate curve $Q_k(t) = \oint_{A_k} < \mathbf{v}(\mathbf{x}, t), \mathbf{n}_k > d\mathbf{x}$.
6) Extract PWV c from the flow rate curves $Q_k(t)$.

Table 1. PWV computation method.

3. Materials

3.1. Digital phantom

Phantoms are essential for the verification of the method and the implementation, due to the difficulties of assessing a reliable ground truth for the PWV in in-vivo measurements. At a first glance, physical (hardware) phantoms might seem to be the best choice. However, for a PWV hardware phantom, design, building, and scanning is complex and costly. In addition, even physical phantoms necessarily contain simplifications and idealizations. Therefore, and as we needed a phantom where the true PWV is a priori known by construction, we opted for a digital phantom in this study.

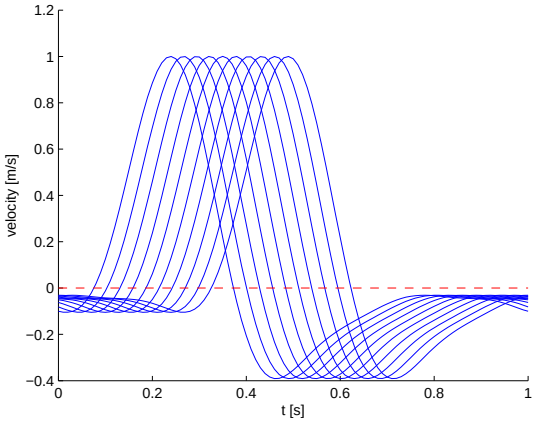

Figure 2. Synthetic flow rate curves $u(z, t)$.

We constructed the digital phantom by combining a stationary Poiseuille flow with a time-dependent scalar component. The time-dependent scalar component was constructed by superposing four Fourier harmonics (adapted from [4], p.126)

$$u(t) = 0.0735 + \sum_{k=1}^{4} A_k \cos\left(k\omega t - \phi_k\right) \qquad (1)$$

with ω as the fundamental frequency (in rad/s), magnitudes $A_1 = 0.3674, A_2 = 0.3564, A_3 = 0.1727, A_4 = 0.0514$ and phases $\phi_1 = -1.01, \phi_2 = -2.64, \phi_3 = 2.16, \phi_4 = 0.75$. From $u(t)$ a spatio-temporal traveling wave packet was formed by letting:

$$u(z, t) = u(t - z/c) \qquad (2)$$

with c as the wave packet velocity (Fig. 2) [1] . As this wave packet travels with constant speed c, also its foot point travels with this speed. Therefore, the PWV according to the TTF criterion is the a priori known parameter c.

The time-dependent velocity field $\mathbf{v}(\mathbf{x}, t)$ of the digital phantom was formed by multiplying $u(z, t)$ with a

[1]This phantom did not include dissipation or reflection effects. We were interested in validating our implementation, and not in a systematic comparison of different PWV extraction algorithms, so this idealized scenario was sufficient for our purposes.

parabolic shaped Poiseuille flow profile in a rigid tube geometry:

$$\mathbf{v}(\mathbf{x},t) = u(z,t)v_{\max}(1-(r/R)^2)\mathbf{e}_z \qquad (3)$$

where $v_{\max}$ is the maximum velocity, $r = \sqrt{x^2+y^2}$, R is the tube radius, and $\mathbf{e}_z$ is the unit vector in z-direction.

We chose parameter values typical for the aorta: the tube radius R is 12 mm, the in-plane resolution is 1 mm, the maximum fluid velocity 1.5 m/s, and the tube length is 30 cm. The PWV c was set to 4.5 m/s, the duration of one heart cycle is 1 s, and the temporal resolution is 40 ms.

Generation of synthetic datasets: To simulate the measurement errors arising from the scanning process, white Gaussian noise was superimposed on the non-stationary velocity field (3). We assumed the tube of the phantom to be embedded into a gel-like substance, with a similar contrast to water. Thus, we were able to use the "additive Gaussian" high-SNR approximation for the velocity noise [5]. The standard deviation σ_{vel} of the velocity is given by the formula [5]:

$$\sigma_{\text{vel}} = \frac{\sqrt{2}}{\pi}\frac{v_{\text{enc}}}{SNR} \qquad (4)$$

with SNR as the signal-to-noise ratio and v_{enc} as the encoding velocity. Heuristically, SNR is around 10 for the aorta [5], and with a reasonable value of v_{enc} = 1.5 m/s we obtained for the standard deviation of the velocity the numerical value σ_{vel} = 6.75 cm/s.

To further keep things simple, we also assumed statistical independence of the noise among the velocity components.

3.2. In-vivo data

To evaluate our PWV implementation on in-vivo data, we obtained 4D PCMRA datasets of 12 young volunteers (average age 24.5 years). These datasets were directly taken from the previously cited study [1], allowing a direct comparison. Measurements were performed on a Siemens TRIO scanner (3 Tesla), using a velocity-encoded phase contrast gradient echo sequence with prospective ECG gating. Scan parameters were spatio-temporal resolution = 1.7 mm x 2.0 mm x 2.2 mm x 42.8 ms, TE = 2.6-3.5 ms, TR = 5.1-6.1 ms, flip angle = 7-15°, and v_{enc} = 1.50 m/s.

4. Results

4.1. Digital phantom

Using the digital phantom, we have investigated accuracy and reproducibility of our PWV computation method. In a Monte Carlo experiment, we generated 100 synthetic datasets of the non-stationary velocity field (3), contaminated with random noise according to the above additive Gaussian noise model. We then applied the PWV calculation algorithm to the synthetic datasets. In the PWV computation, we set the spatial distance to Δs to 1 cm and shrunk the mask to $\epsilon = 95\%$ of it's original size (these values were also used in the remainder of the paper). We obtained 4.5095 m/s $\pm$ 0.02688 m/s as the mean value and the standard deviation for the PWV.

Observer	Mean PWV $\pm$ standard deviation
1	4.46 m/s $\pm$ 0.35 m/s
2	4.58 m/s $\pm$ 0.43 m/s
Markl et al. [1]	4.39 m/s $\pm$ 0.32 m/s

Table 2. PWV statistics.

4.2. In-vivo data

We preprocessed the data using the workflow described in [3] (data import, correction of velocity offset errors, phase unwrapping and semiautomatic segmentation of the aorta).

Two observers then independently measured the PWV on the preprocessed and segmented in-vivo datasets. PWV measurement was done by placing the start point into the aorta ascendens (after the aortic bulb) and the end point into the aorta descendens as distal as possible. The PWV algorithm then computed PWV according to the time-to-foot (TTF) criterion [1].

We further note that both observers worked on the same preprocessed and segmented data. This arrangement was chosen to assess the variability of the PWV computation itself (depending on the location of the measurement planes etc), not the contribution of preprocessing and segmentation done by different observers.

PWV measurements: The mean and standard deviation for the PWV TTF measurements of the two observers and the corresponding results from [1] are shown in Table (2). For comparing the PWV values from Table (2), it is more appropriate to look at the relative differences $2|E_1 - E_2|/|E_1 + E_2|$, rather than their absolute differences. According to this, the relative difference between the PWV of observer 1 and the PWV from [1] is 1.6%, between observer 2 and [1] is 4.2%, and between the two observers is 2.7%.

Bland-Altman for PWV: To further analyze the agreement between the two observers, the Bland-Altman method was used [6]. The Bland-Altman plot is shown in Figure (3). The plot allows us to investigate the existence of any systematic bias between the observers and to identify possible outliers. We found a small bias of 0.12 m/s $\pm$ 0.13 m/s, and a maximum discordance of 0.35 m/s between the observers (still within the 95% confidence inter-

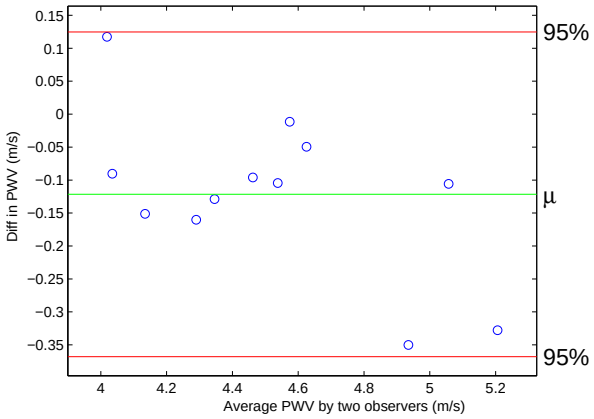

Figure 3. Bland-Altman plot for the two observers PWV.

val). This maximum discordance corresponds to a relative difference between the two observers of 7.1%.

The presence of a fixed systematic bias between the two observers was further analyzed using a one-sample t-test. For the null hypothesis of no fixed bias between the two observers, we computed the p-value (observed significance level) to be 0.65%. This is nonsignificant at the usual significance level of 5%.

Time measurements: Mean time per case for preprocessing and segmentation was 30 minutes, and 4 minutes for PWV measurement.

5. Discussion

The Monte Carlo experiment on the digital phantom gives evidence to the high accuracy of our PWV computation scheme. The low standard deviation obtained in the experiment demonstrates a high reproducibility.

For the in-vivo data, the results of the two observers were in good accordance with the results from Markl et al [1].

Comparing the mean and standard deviation of the computed PWVs in each group with [1] as the benchmark, we found that the method gives an accuracy comparable to [1], as the relative errors between the two observers and [1] are small. The same conclusion applies with respect to reproducibility.

The Bland-Altman analysis demonstrated a bias of 0.1216 m/s between the two observers. As already established above, the corresponding relative error is small, so the observers were in good accordance. Also, the presence of statistical outliers could not be established, because the two measurements with maximum deviation were inside the 95% confidence limits. The maximal discordance between the two observers was 0.3501 m/s, corresponding to the relative difference 7.1%. In this case, the two observers had placed the starting point in different ways. Using a one-sample t-test, we were unable to establish the existence of a systematic bias between the two observers. This might be partly due to the low level of the bias, but also to the small sample size (n=12) available in the study. We believe that the placing of the starting point has the most pronounced effect on the bias.

As the total time is 34 minutes per case, the tremendous time saving is apparent when compared with the study of Markl et al [1]. Markl et al. used a combination of Matlab scripts and Ensight3D, plus a very time consuming manual placement of planes and manual segmentation, resulting in a processing time of approximately 3 hours per case. In contrast, our solution is completely integrated and largely automatized. As a result, this allows faster data analysis and thus the application in large-scale clinical studies.

6. Conclusion

Comparing our PWV results to those of Markl et al. (PWV 4.39 m/s $\pm$0.32 m/s), we find that our method gives similar accuracy and reproducibility, but at a significantly reduced processing time.

References

[1] Markl M, Wallis W, Brendecke S, Simon J, Frydrychowicz A, Harloff A. Estimation of Global Aortic Pulse Wave Velocity by Flow-Sensitive 4D MRI. Magnetic Resonance in Medicine 2010;63:1575–1582.

[2] Westenberg J, de Roos A, Grotenhuis H, Steendijk P, Hendriksen D, van den Boogaard P, van der Geest R, Bax J, Jukema JW, Reiber J. Improved Aortic Pulse Wave Velocity Assessment From Multislice Two-Directional In-Plane Velocity- Encoded Magnetic Resonance Imaging. Journal of Magnetic Resonance Imaging 2010;32:1086–1094.

[3] Hennemuth A, Friman O, Schumann C, Bock J, Drexl J, Huellebrand M, Markl M, Peitgen HO. Fast Interactive Exploration of 4D MRI Flow Data. In SPIE Medical Imaging Conference 2011. 2011; 1–8.

[4] Caro C, Pedley T, Schroeter R, Seed W. The Mechanics of the Circulation. Cambridge University Press, 2012.

[5] Friman O, Hennemuth A, Harloff A, Bock J, Mark M, Peitgen HO. Probabilistic 4D Blood Flow Tracking and Uncertainty Estimation. Medical Image Analysis 2011;15:720–728.

[6] Bland JM, Altman DG. Statistical methods for assessing agreement between two methods of clinical measurement. Lancet 1986;327:307–310.

Address for correspondence:

Johann B. Drexl
Fraunhofer MEVIS, Bremen, Germany.
Johann.Drexl@ieee.org